

Thickness-dependent magnetic property of FeNi thin film grown on flexible graphene substrate

Suixin Zhan(詹遂鑫), Shaokang Yuan(袁少康), Yuming Bai(白宇明), Fu Liu(刘福), Bohan Zhang(张博涵), Weijia Han(韩卫家), Tao Wang(王韬), Shengxiang Wang(汪胜祥), and Cai Zhou(周偲)

Citation: Chin. Phys. B, 2025, 34 (**2**): 027503. DOI: 10.1088/1674-1056/ad92fd
Journal homepage: http://cpb.iphy.ac.cn; http://iopscience.iop.org/cpb

What follows is a list of articles you may be interested in

Simulation of magnetization process and Faraday effect of magnetic bilayer films

Sheng Gao(高升), An Du(杜安), Lei Zhang(张磊), Tian-Guang Li(李天广), and Da-Cheng Ma(马大成)
Chin. Phys. B, 2024, 33 (**9**): 097505. DOI: 10.1088/1674-1056/ad5a76

Enhanced resonance frequency in Co_2FeAl thin film with different thicknesses grown on flexible graphene substrate

Cai Zhou(周偲), Shaokang Yuan(袁少康), Dengyu Zhu(朱登玉), Yuming Bai(白宇明), Tao Wang(王韬), Fufu Liu(刘福福), Lulu Pan(潘禄禄), Cunfang Feng(冯存芳), Bohan Zhang(张博涵), Daping He(何大平), and Shengxiang Wang(汪胜祥)
Chin. Phys. B, 2024, 33 (**3**): 037506. DOI: 10.1088/1674-1056/acfafa

Effect of seed layers on the static and dynamic magnetic properties of CoIr films with negative effective magnetocrystalline anisotropy

Tianyong Ma(马天勇), Sha Zhang(张莎), Chenhu Zhang(张晨虎), Zhiwei Li(李志伟), Tao Wang(王涛), and Fashen Li(李发伸)
Chin. Phys. B, 2023, 32 (**12**): 127503. DOI: 10.1088/1674-1056/acd523

In-plane spin excitation of skyrmion bags

Shuang Li(李爽), Ke-Xin Li(李可欣), Zhao-Hua Liu(刘照华), Qi-Yuan Zhu(朱起源), Chen-Bo Zhao(赵晨博), Hu Zhang(张虎), Xing-Qiang Shi(石兴强), Jiang-Long Wang(王江龙), Rui-Ning Wang(王瑞宁), Ru-Qian Lian(连如乾), Peng-Lai Gong(巩朋来), and Chen-Dong Jin(金晨东)
Chin. Phys. B, 2023, 32 (**11**): 117503. DOI: 10.1088/1674-1056/acd327

Angular control of multi-mode resonance frequencies in obliquely deposited CoZr thin films with rotatable stripe domains

Chao-Zhong Li(李超众), Chang-Jun Jiang(蒋长军), and Guo-Zhi Chai(柴国志)
Chin. Phys. B, 2021, 30 (**3**): 037502. DOI: 10.1088/1674-1056/abccb4

Thickness-dependent magnetic property of FeNi thin film grown on flexible graphene substrate

Suixin Zhan(詹遂鑫)[1,2], Shaokang Yuan(袁少康)[1,2], Yuming Bai(白宇明)[3], Fu Liu(刘福)[4], Bohan Zhang(张博涵)[1,2], Weijia Han(韩卫家)[1,2], Tao Wang(王韬)[3], Shengxiang Wang(汪胜祥)[1,2,†], and Cai Zhou(周偲)[1,2,‡]

[1] *State Key Laboratory of New Textile Materials and Advanced Processing Technologies, Wuhan Textile University, Wuhan* 430200, *China*
[2] *School of Mathematical and Physical Sciences, Wuhan Textile University, Wuhan* 430200, *China*
[3] *School of Integrated Circuits, Huazhong University of Science and Technology, Wuhan* 430074, *China*
[4] *Key Laboratory for Magnetism and Magnetic Materials, Ministry of Education, Lanzhou University, Lanzhou* 730000, *China*

(Received 16 August 2024; revised manuscript received 9 October 2024; accepted manuscript online 15 November 2024)

Electronics over flexible substrates offer advantages of flexibility, portability and low cost, and promising applications in the areas of energy, information, defense science and medical service. In recent years, tremendous progress has been witnessed in the development of flexible wearable devices that can be potentially massively deployed. Of particular interest are intelligent wearable devices, such as sensors and storage cells, which can be integrated by flexible magnetoelectronic devices based on magnetic thin films. To examine this further, the magnetic properties of FeNi thin films with different thicknesses grown on flexible graphene substrate are investigated at room temperature. The coercivity increases with increasing thicknesses of FeNi thin film, which can be attributed to the increase of grain size and decrease of surface roughness. Moreover, the thickness modulated magnetic property shows a magnetic anisotropy shift increase with varying thicknesses of FeNi thin film by using measurements based on ferromagnetic resonance, which further enhances the resonance frequency. In addition, the resonance peak is quite stable after bending it for ten cycles. The result is promising for the future design of flexible magnetoelectronic devices.

Keywords: resonance frequency, FeNi thin film, flexible graphene substrate, magnetic property

PACS: 75.70.–I, 76.50.+g, 32.30.Dx

DOI: 10.1088/1674-1056/ad92fd **CSTR:** 32038.14.CPB.ad92fd

1. Introduction

Along with the rapid development and continual increase of information data in microwave technologies, soft magnetic materials used as imperative functional materials for information processing and storage have become an incredible cornerstone of modern information society.[1–3] Magnetic anisotropy,[4–6] one of the important intrinsic parameters for soft magnetic materials, determines the coercive field and magnetic moment orientation, which can influence the operating frequency and even power consumption. Thus, the investigations of mediation methods and the mechanism of magnetic anisotropy are essential issues in soft magnetic materials. Fan *et al*. have reported in-plane uniaxial magnetic anisotropy mediated by an oblique sputtering angle during sputtering in soft magnetic thin film grown on a Si substrate, which leads to an increase of resonant frequency.[7] We have investigated an electric-field control of magnetic anisotropy modulation in an epitaxial magnetic thin film on a $Pb(Mg_{1/3}Nb_{2/3})O_3$–$30\%PbTiO_3$ substrate.[8] Although the magnetic anisotropy of magnetic thin film can be modified by the methods of changing the oblique sputtering angle and the applied electric field, the point of rigid substrate inevitably impedes the flexible electronic device performances. Recently, flexible materials have been exploited to implement functionalities on flexible electronic devices, which exhibit more favorable properties than most of the rigid substrates in terms of weight saving, flexibility, mechanical reliability and excellent environmental toughness.[9–13] For example, Liu *et al.* have demonstrated a self-assembled periodic wrinkling surface structure in CoFeB thin films grown on polydimethylsiloxane membranes induced by applying uniaxial tensile strains to continuously tune high frequency magnetic properties.[14] Graphene film as another flexible substrate, compared with a polydimethylsiloxane substrate, has significant advantages, including high conductivity, mechanical strength, thermal stability, surface area, environmental friendliness, processability and biocompatibility.[15,16] He's group has reported a flexible graphene film for radio-frequency antennas, multi-beam radiation, highly sensitive wearable sensors, etc.[17–19] In fact, graphene film as a flexible substrate is expected to spark a number of studies into flexible magnetoelectronic devices. In addition, FeNi thin film has received great attention due to its highly sought-after magnetic characteristics such as high saturation magnetization, which can be widely used in static and high-frequency for soft mag-

†Corresponding author. E-mail: shxwang@wtu.edu.cn
‡Corresponding author. E-mail: szhou@wtu.edu.cn

© 2025 Chinese Physical Society and IOP Publishing Ltd. All rights, including for text and data mining, AI training, and similar technologies, are reserved.

netic materials. Therefore, in this work, we report on the thickness-dependent magnetic property of FeNi thin film with different thicknesses grown on a flexible graphene substrate (FGS). With increasing thicknesses of the FeNi thin film, the grain continues to grow and the corresponding size becomes larger, which leads to the increase of coercivity. Meanwhile, the magnetic anisotropy — using measurements based on the ferromagnetic resonance (FMR) — increases, and the resonance peak is quite stable despite bending it for ten cycles. Moreover, different thicknesses of FeNi thin films grown on FGS realize an increase of resonance frequency from 3.8 GHz to 4.1 GHz and a decreasing trend of the permeability.

2. Experiments

FeNi thin films with different thicknesses of 70 nm, 140 nm, 210 nm, and 280 nm, respectively, are deposited by radio frequency (RF) magnetron sputtering on the FGS at a common base pressure of 8×10^{-4} Pa and work processing Ar pressure of 1 Pa and a power of 50 W, the thickness of the FGS is 100 μm. A field emission scanning electron microscope (SEM, Hitachi SU5000) is employed to observe the cross-section of the microstructures. The surface roughness is measured by an atomic force microscope (AFM) using an Asylum Research © MFP-3D. The x-ray diffraction (XRD) measurements are performed on an X'Pert x-ray powder diffractometer with Cu $K\alpha$ radiation (1.54056 Å). The FMR measurements are carried out with a PNA 8722ES vector network analyzer using the coplanar waveguide method. Permeability spectra are carried out with a PNA E8363B vector network analyzer using the microstrip method. An upright metallurgical microscope (Soptop RX50M) is employed to observe the surface morphology microstructures.

3. Results and discussion

In the FeNi/FGS structure, the in-plane magnetic hysteresis loop of the sample with a thickness of 70 nm is shown in Fig. 1(a). It exhibits a weak in-plane magnetic uniaxial anisotropy, which can be attributed to the oblique sputtering. The slight oblique columnar structure is observed by a SEM cross-section image (see the inset in Fig. 1(a)), which indicates the good quality of FeNi thin film grown on the FGS. Similar results can also be obtained in samples with FeNi film thicknesses of 140 nm, 210 nm and 280 nm. The saturate magnetic field H_s and coercivity H_c are extracted from these magnetic hysteresis loops, as shown in Fig. 1(c). With increasing thicknesses of FeNi thin film, H_s and H_c increase from 370 Oe to 1210 Oe and from 46 Oe to 78 Oe, respectively, as shown in Fig. 1(b), which may be caused by the increase of grain size. This can be proved by XRD results in the following section.

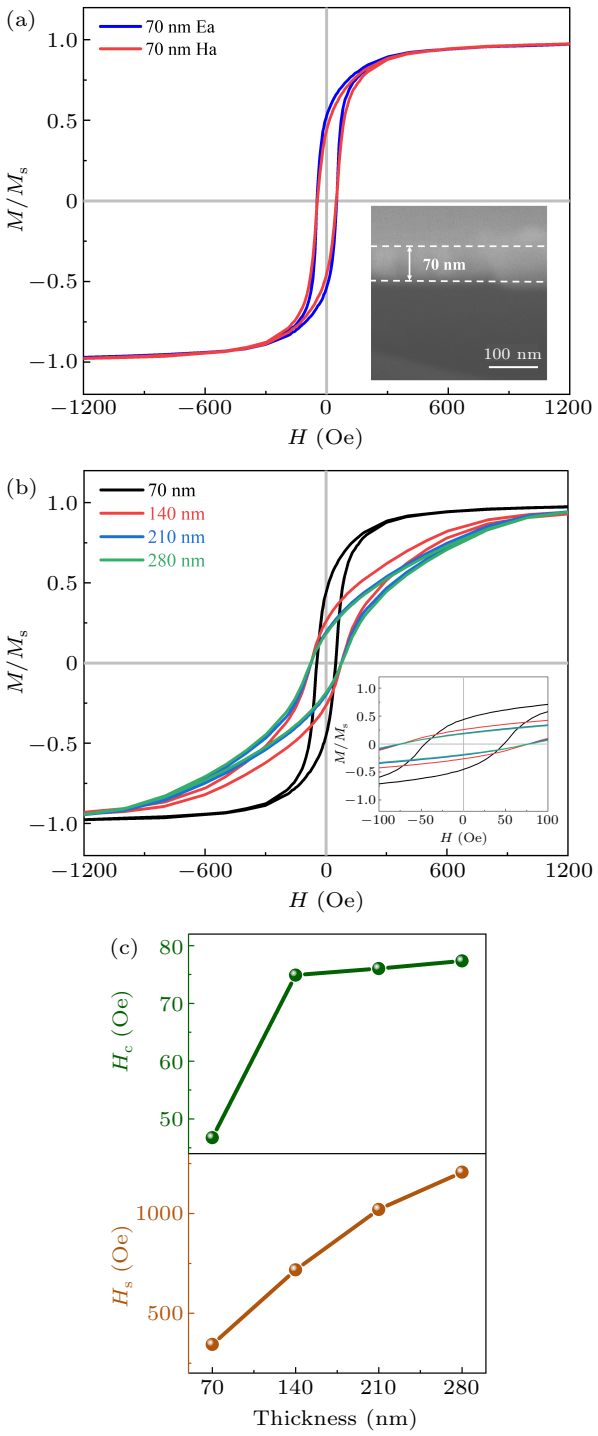


Fig. 1. (a) The in-plane magnetic hysteresis loop of FeNi thin film with a thickness of 70 nm at easy and hard axes. (b) The in-plane magnetic hysteresis loop of FeNi thin film with different thicknesses at the hard axis. (c) Two curves of H_c and H_s changing with thicknesses, respectively.

Figure 2(a) presents the crystal structures of FeNi/FGS samples. The sharp diffraction peak (004) of the FGS is located at 54.5°. The (111) peak of FeNi thin film appears at 44.2°, which indicates the polycrystalline feature of FeNi thin film grown on the FGS. The intensity of the (111) peak increases with the increasing thickness of the FeNi thin film, which implies an enhancement of the crystallization. Moreover, the width of the peaks decreases as thicknesses increase, revealing the increase of the grain size. According to the

Scherrer equation, grain sizes of FeNi thin films are indeed denoted as increasing from 8.3 nm to 11.9 nm with increasing thickness of FeNi thin films from 70 nm to 280 nm, which is consistent with the result of H_c obtained from VSM measurement. In addition, the surface roughness values, measured by the AFM, decrease from 15 nm to 7 nm, as shown in Fig. 2(b). By increasing the thickness of the FeNi thin film, the grain size increases, as shown in Fig. 2(a), which indicates that less grain boundary will be produced. This result can lower the magnetic moment's scattering in the FeNi thin film and make the magnetic moment align in one direction easier, further leading to the increase of the coercivity of FeNi thin film. Generally, the less the grain boundary, the more the microstructural defects are reduced.[20] Moreover, internal stresses usually develop around the grain boundary. Considering the decrease of the grain boundary with the increasing thickness of the FeNi thin film, the total internal stress might decrease.[21] It can be beneficial to keep the magnetization direction of the magnetic moment, which leads to the large magnetization reversal magnetic field. According to the above results and the random anisotropy model,[22] this result can influence the dynamic magnetic properties of the FeNi thin film grown on FGS, which will be discussed in detail below.

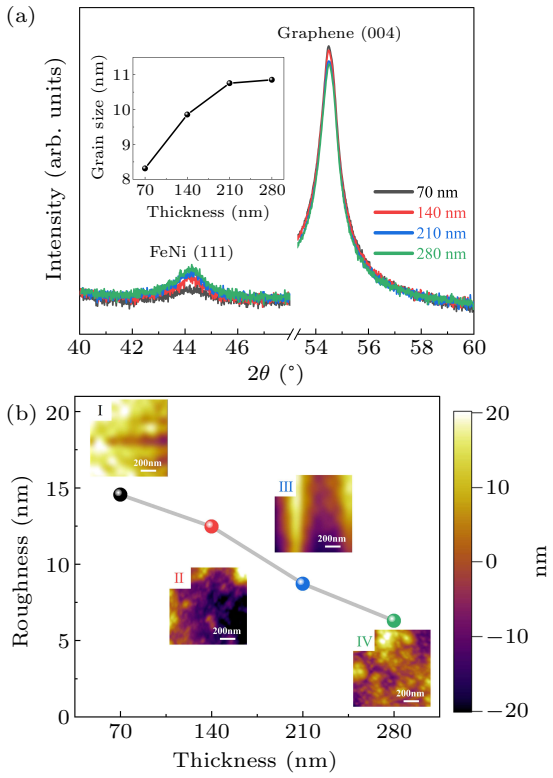


Fig. 2. (a) XRD patterns of FeNi thin film with different thicknesses. The inset shows the change of grain size with thicknesses of FeNi thin film. (b) The change of surface roughness with thicknesses of FeNi thin film. The inset shows the morphology of these samples measured by the AFM.

Generally, magnetic thin film applications are based on analyses of dynamic magnetic or magnetization processes. Moreover, the effect of magnetic interactions is much more salient in high-frequency magnetization dynamics due to the nonlinear effect, particularly at magnetic resonance frequencies. In order to investigate the thickness-dependent magnetic anisotropy for these samples of FeNi/FGS, the dynamic magnetic property is measured by FMR using a vector network analyzer with a coplanar waveguide method. Figure 3(a) shows the schematic illustration of FMR. For 210 nm-thick FeNi thin film, the typical FMR spectra are obtained as shown in Fig. 3(b) (solid dots). In general, the magnetization is probed by using a special phase correlation under the microwave excitation; the FMR spectrum does not correspond to the imaginary part of the susceptibility alone, but in fact represents a mixture of the imaginary and real parts. Therefore, the actual function of the absorption curve can be fitted by an asymmetric Lorentzian function[23]

$$\varphi(H) = A\frac{\Delta H\cos\theta + (H - H_r)\sin\theta}{\Delta H^2 + (H - H_r)^2}, \tag{1}$$

where H is the external magnetic field, H_r is the magnetic resonance field, ΔH is the half-width at half-maximum of the linewidth, θ is the phase that mixes the real and imaginary parts of the dynamic susceptibility, and A is the integral coefficient. Figure 3(b) shows the result of fitting of the FMR curves using Eq. (1) (silver lines). The resonant magnetic field increases from 467 Oe to 1957 Oe as the micro frequency increases from 6 GHz to 12 GHz for 210 nm-thick FeNi thin film. Similar results can be obtained for all thin films. As a result, figure 3(c) shows the data of frequency-dependent H_r under different thicknesses of FeNi thin film (solid dots), which is fitted by using Kittel's equation[24]

$$f = \frac{\gamma}{2\pi}\sqrt{(H_r + H_k)(H_r + H_k + 4\pi M_{eff})}, \tag{2}$$

where the gyromagnetic ratio $\gamma/2\pi = 2.8$ GHz/kOe, $4\pi M_{eff}$ is the effective magnetization, and H_k is the in-plane magnetic uniaxial anisotropy field. Figure 3(d) shows the corresponding fitting curves (silver lines). Meanwhile, the values of $4\pi M_{eff}$ and H_k can be extracted by fitting frequency-dependent H_r curves using Eq. (2). $4\pi M_{eff}$ appears to remain almost constant as the thickness of FeNi thin film increases from 70 nm to 280 nm. However, H_k obviously increases from 103 Oe to 186 Oe with increasing thicknesses of FeNi thin films. These results can be explained by the increase of the FeNi grain size with increasing thicknesses of FeNi thin films. This result can lead to the increase of resonance frequency.

The dependence of permeability on the frequency with different thicknesses of FeNi thin films is measured by a vector network analyzer with the microstrip method. Figures 4(a) and 4(b) show the dynamic real part μ' and imaginary part μ'' of the complex permeability spectra of FeNi thin film measured at 200 Oe magnetic field ranging from 1 GHz to 9 GHz. The real part μ' exhibits a dispersive-type curve, while

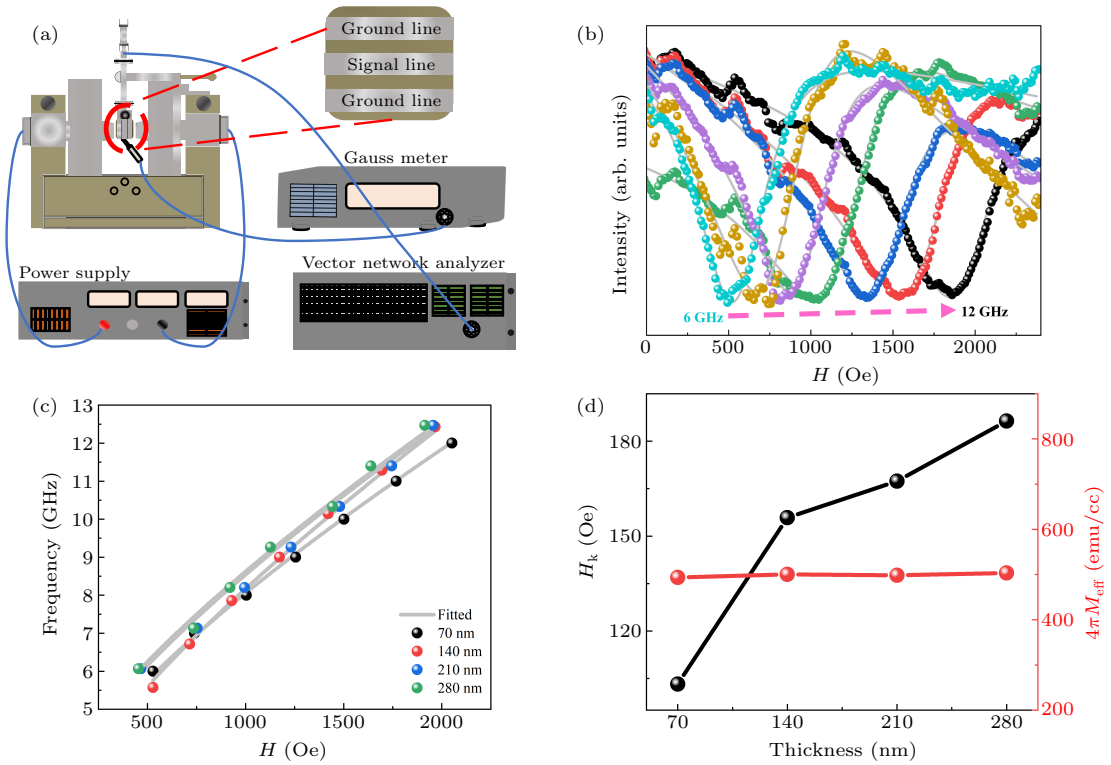


Fig. 3. (a) Schematic illustration of FMR using a vector network analyzer. (b) Experimental data (dots) and fitting curves (lines) of FMR for 210 nm-thick FeNi thin film. (c) The applied microwave frequency versus the resonance magnetic field with different thicknesses of FeNi thin film. (d) The change of H_k and $4\pi M_{eff}$ with different thicknesses of FeNi thin film.

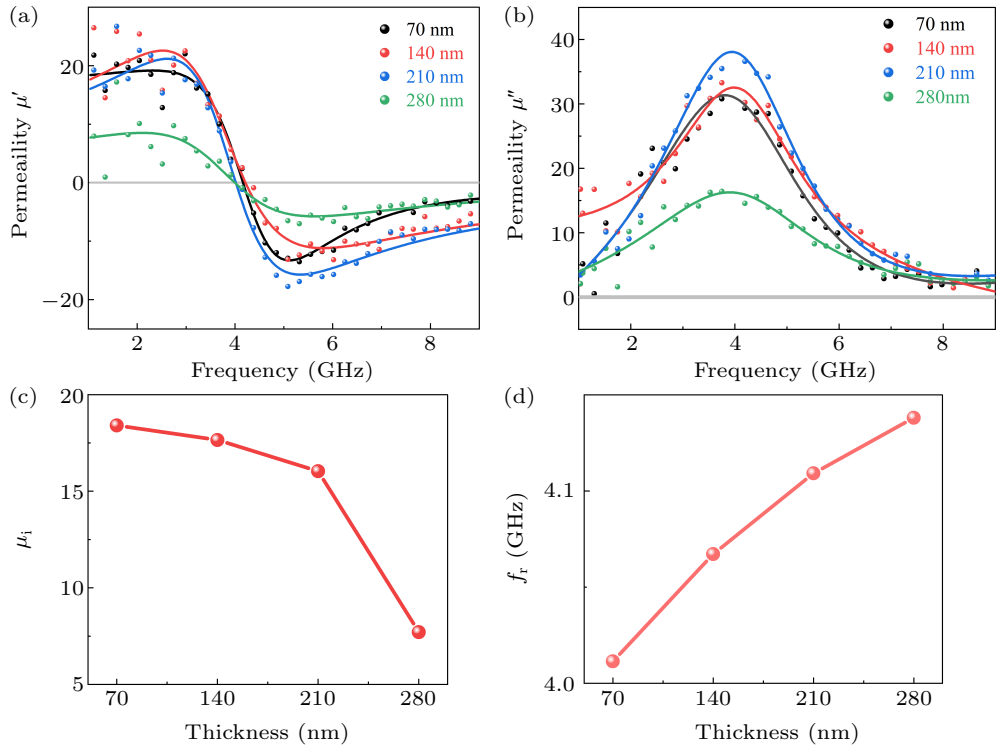


Fig. 4. (a) The dynamic real part μ' and (b) imaginary part μ'' of complex permeability spectra of FeNi thin film. The change of (c) permeability μ_i and (d) resonance frequency peak with thicknesses of FeNi thin film.

a Lorentzian shape resonance curve is shown for imaginary part μ'', which reveals a typical resonance permeability spectrum. The permeability μ_i decreases with increasing thicknesses of FeNi thin films, as shown in Fig. 4(c). However, the imaginary permeability spectra of FeNi thin film with increasing thicknesses from 70 nm to 280 nm display clear resonance frequency peaks, increasing from 3.8 GHz to 4.1 GHz (Fig. 4(d)). These results are consistent with the results of H_k-dependent thickness of FeNi thin films, and further confirm that the thickness of FeNi thin film grown on FGS can mediate

the magnetic property. In flexible magnetoelectronic apparatus, the permeability of magnetic thin film can directly determine the performance and sensitivity of magnetic devices. In magnetic devices such as antennas and sensors, magnetic thin film is used to detect subtle changes in the magnetic field. The high permeability of magnetic thin film can lessen the hysteresis loss and eddy current loss, further helping to improve the sensitivity and resolution of magnetic devices. This result can strengthen the accuracy of the detection of magnetic field intensity for sensors and enhance signal transmission efficiency for antennas. In this work, with decreasing thicknesses of FeNi thin film, a high permeability is obtained, which can satisfy the need for high sensitivity of magnetic devices. However, high resonance frequency can only be gained by increasing the thickness of the FeNi thin film; this is a persistent requirement for the increase of work frequency in communication equipment. In fact, the preferred approach to the higher resonance frequency and/or higher permeability is dependent on the application scene.

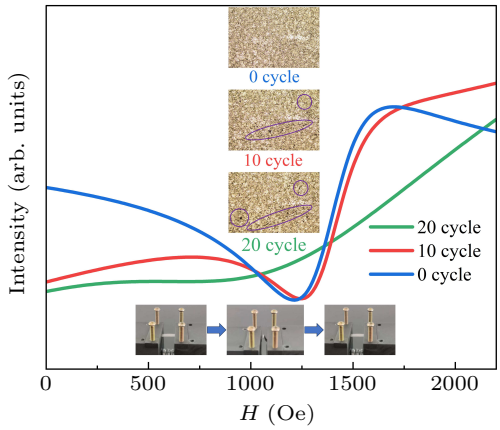


Fig. 5. Curves produced under an unfolded state and after being folded for ten cycles and twenty cycles. The top inset shows more cracks with increasing folding cycles. The bottom inset shows the folding schematic diagram.

To verify the performance of the FeNi thin film after mechanical bending, the sample of FeNi (210 nm)/FGS is placed on a customized automatic counting slide rail, and tested after different bending cycles, as shown in Fig. 5. The FMR curves begin to deform after bending for ten cycles, whereas cracks can be observed and an obvious resonance peak is obtained. With increasing bending to twenty cycles, more cracks can be seen, while the resonance peaks disappear. Cracks in metal films appeared inside large grains and between small grains,[25] which can influence the grain size and magnetic resonance property. The cracks may lead to the disappearance of the resonance field's peak in FeNi thin film in this work. The above results are obtained under a bending speed of 1 s per cycle. When the bending speed increases to 10 s per cycle, a similar result can be observed.

4. Conclusion

In summary, we have identified the microstructure and dynamic magnetic property of FeNi thin film with different thicknesses grown on FGS. With increasing thicknesses of FeNi thin film, the magnetic anisotropy is demonstrated to increase by measurement of the FMR. This result can be attributed to the crystal structure of FeNi thin film with different thicknesses. Moreover, the resonance peak is quite stable after bending for ten cycles. In addition, a clear resonance peak of FeNi thin film changing from 3.8 GHz to 4.1 GHz and a decrease of permeability are obtained. These results remove the obstacles of transmission distance and the signal quality of communication systems.

Acknowledgments

Project supported by the National Natural Science Foundation of China (Grant Nos. 51901163 and 12104171), the Fundamental Research Funds for the Central Universities (Grant No. 2021XXJS025), and the Natural Science Foundation of Hubei Province (Grants No. 2024AFB888).

References

[1] Fish G E 1990 *Proc. IEEE* **78** 947
[2] Arai K I and Ishiyama K 1994 *J. Magn. Magn. Mater.* **133** 233
[3] Silveyra J M, Ferrara, Huber E D L and Monson T C 2018 *Science* **362**
[4] Meiklejohn W H and Bean C P 1957 *Phys. Rev.* **105** 904
[5] Johnson M T, Bloemen P J H, den Broeder F J A and de Vries J J 1996 *Rep. Prog. Phys.* **59** 1409
[6] Xue D S, Li F S, Fan X L and Wen F S 2008 *Chin. Phys. Lett.* **25** 4120
[7] Fan X L, Xue D S, Lin M, Zhang Z M, Guo D W, Jiang C J and Wei J Q 2008 *Appl. Phys. Lett.* **92** 222505
[8] Zhou C, Shen L K, Liu M, Gao C X, Jia C L, Jiang C J and Xue D S 2018 *Adv. Funct. Mater.* **28** 1707027
[9] Liu W L, Ao D, Liu C J, Wang X, Dong S H, Ren H J, Xia A and Tang G Q 2022 *J. Magn. Magn. Mater.* **551** 169134
[10] Zhao S S, Zhou Z Y, Li C L, Peng B, Hu Z Q and Liu M 2018 *ACS Nano* **12** 7167
[11] Lu L J, Ding W Q, Liu J Q and Yang B 2020 *Nano Energy* **78** 105251
[12] Matsumoto H, Ota S, Koyama T and Chiba D 2021 *Appl. Phys. Lett.* **118** 022406
[13] Zhang H, Li Y Y, Yang M Y, Zhang B, Yang G, Wang S G and Wang K Y 2015 *Chin. Phys. B* **24** 077501
[14] Liu J, Chen J N, Zhang Y R, Fu S J, Chai G Z, Cao C M, Zhu X Y, Guo Y B, Cheng W J, Jiang D M, Zhao Z J and Zhan Q F 2021 *ACS Appl. Mater. & Inter.* **13** 29975
[15] Wang Y F, Zhang Q, Xu H M, Xi G, Chang Y H, Zhang J R, He X D, Zuo Y L, Cui B S and Xi L 2024 *Chin. Phys. Lett.* **41** 067502
[16] Zhou C, Yuan S K, Zhu D Y, Bai Y M, Wang T, Liu F F, Pan L L, Feng C F, Zhang B H and He D P 2024 *Chin. Phys. B* **33** 037506
[17] Fan C, Wu B, Song R G, Zhao Y T, Zhang Y H and He D P 2019 *Carbon* **155** 506
[18] Song R G, Mao B Y, Wang Z, Hui Y Y, Zhang N, Fang R, Zhang J W, Wu Y, Ge Q, Novoselov K S and He D P 2023 *PNAS* **120** e2209807120
[19] Qian W, Fu H Q, Sun Y, Wang Z, Wu H, Kou Z K, Li B W, He D P and Nan C W 2022 *Adv. Mater.* **34** 2206101
[20] Liu W, Liu N J, Ji S L, Hua H F, Ma Y H, Hu R Y, Zhang J, Chu L, Li X A and Huang W 2020 *Nano-Micro Lett.* **12** 119
[21] Zhang S L, Zhan Q F, Yu Y, Liu L P, Li H H, Yang H L, Xie Y L, Wang B M, Xie S H and Li R W 2016 *Appl. Phys. Lett.* **108** 102409
[22] Herzer G 1990 *IEEE Trans. Magn.* **26** 1397
[23] Mecking N, Gui Y S and Hu C M 2007 *Phys. Rev. B* **76** 224430
[24] Kittel C 1948 *Phys. Rev* **73** 155
[25] Kraft O, Schwaiger R and Wellner P 2001 *Mat. Sci. Eng. A* **319** 919